Validation of Density Functional Methods for the Calculation of Small Gold Clusters

Yuan-Kun Shi, Zhen Hua Li,* and Kang-Nian Fan

Department of Chemistry, Shanghai Key Laboratory of Molecular Catalysts and Innovative Materials, Fudan University, Shanghai 200433, People's Republic of China

Received: June 14, 2010; Revised Manuscript Received: August 5, 2010

The performance of various density functional theory methods on the geometries and energetics of Au_2, Au_3, Au_4, and Au_5 has been systematically evaluated. The results were compared with those from experiments or high-level wave function theory methods. In the present study, spin−orbit (SO) coupling was considered. It was found that SO coupling plays a very important role in the calculation of both the atomization energies and relative stability of the isomers of gold clusters. Functionals including SO coupling effect will overestimate the atomization energies of gold clusters compared with those just including the scalar relativistic (SC) effect. On the other hand, hybrid functionals will underestimate the atomization energies compared with those of the corresponding pure functionals. For the calculation of the relative stability of the different isomers, many functionals not including SO coupling will predict the wrong stability order. In addition, SO correction to the atomization energy of the cluster (ΔE_{SO}) has a weak dependence on the choice of functional. A linear relationship was established between ΔE_{SO} and the number of Au atoms and Au−Au bonds in the cluster. The relationship indicates that inclusion of SO coupling will favor the isomer with more Au−Au bonds. Among all of the functionals evaluated, the SO TPSSh method has the best overall performance, and SC M06-L also performs well, although it predicts that the two isomers of Au_3 are almost degenerate in energy.

1. Introduction

The application of gold clusters in catalysis has attracted much attention in the past decades.[1−8] As a model catalyst, gold clusters have shown strong potential in many reactions, in both heterogeneous and homogeneous catalysis. Chemists have extensively studied the static properties of the pure gold clusters[9−40] and gold clusters with phosphanes,[41−43] thiolates,[44−50] or halides,[51−54] owing to their importance in the fields of chemistry. The dynamic properties of gold clusters in the catalytic reaction are also important,[55−57] but systematic research studies are still lacking. There may be two reasons for this: (1) Ab initio simulation of gold clusters[58] is accurate but very time-consuming; (2) on the other hand, although quasi-classical dynamics simulation is fast and many works on the analytical potential energy surfaces (PESs) for gold[59−72] have been published, many of these analytical PESs are not accurate enough in studying dynamic properties of gold clusters as they do not take correct many-body effects into consideration. The need to build an accurate PES becomes urgent due to the reasons mentioned above. To build a reliable PES, an accurate and efficient calculation method is required to build a database of the accurate energetic and structural properties of the gold clusters due to the lack of accurate experimental results for them. However, it is difficult to evaluate which computational method is more appropriate for gold clusters, and the experimental data for gold clusters are limited to very small clusters (Au_2[73,74] and Au_3[75]). In the present work, we evaluate the performance of different density functional theory (DFT) methods on the energetic and structural properties of small gold clusters to determine which one is more suitable for the calculation of gold clusters.

* To whom correspondence should be addressed. E-mail: lizhenhua@fudan.edu.cn.

It is widely accepted that relativistic effect is important in the calculation of gold systems.[76−80] Theoretically, the relativistic effect can be calculated by performing four-component,[81] two-component, and scalar relativistic (SC) calculations, which attempt to solve the Dirac−Hartree−Fock equation at various levels of approximation. According to Kullie et al.,[82] calculations including the two-component relativistic spinors, which account for the spin−orbit (SO) coupling effect, and using relativistic effective core potentials (RECPs) are very efficient, and the two-component relativistic spinor method is already implemented in the NWCHEM software package for the DFT methods.[83−85] It has also been pointed out by Rusakov et al.[86] that such techniques can accurately account for the relativistic effect but with acceptable cost. In addition, the utilization of ECP and large valence basis sets provides a practical solution to similar problems, as concluded by Fuentealba and Simón-Manso.[87]

Many theoretical studies have been published on Au_2−Au_{20} and even larger clusters.[1−3,10,88−95] Most of them use DFT methods. However, systematic evaluation of the reliability of the DFT methods for the calculation of gold clusters is scarce in the literature. In this work, the performance of DFT functionals has been evaluated to determine which one gives the best results but with acceptable cost. The effect of SO coupling has also been systematically investigated since only the SC effect is considered in most previous studies. The functionals evaluated include pure GGA functionals (BLYP,[96,97] BP86,[96,98] PBE,[99,100] PW91,[101] FT97,[102,103] B88PW91,[96,101] HCTH series,[104−108] BOP,[109] PBEOP,[110] and $B97^{GGA}$-1[111]), hybrid GGA functionals (B3LYP,[96,97,112,113] BHandHLYP,[96,97,114] ACM,[113] B97 series,[115−117] B98,[118] PBEh,[99,119] and MPW1K[120]), pure meta-GGA functionals (M06-L,[121] TPSS,[122] and PKZB99[123]), and hybrid meta-GGA functionals (M05,[124] M05-2X,[125] M06,[121] M06-2X,[121] M06-HF,[126] VS98,[127] MPW1B95,[128] PWB6K,[129] BB1K,[130] PW6B95,[129] and TPSSh[131]).

10.1021/jp105428b
Published on Web 09/01/2010

TABLE 1: Equilibrium Bond Length (Å) and Cohesive Energy (kcal/mol) of Au_2 Calculated by the SO BP86 and SO TPSSh Methods

valence basis set[a]	bond length		cohesive energy	
	SO BP86	SO TPSSh	SO BP86	SO TPSSh
aug-cc-pVDZ (9s8p7d2f)	2.513	2.504	27.1	25.8
aug-cc-pVTZ (11s10p9d3f2g)	2.501	2.493	28.2	26.8
aug-cc-pVQZ (15s12p11d4f3g2h)	2.502	2.494	27.6	26.2
aug-cc-pV5Z (17s14p12d5f4g3h2i)	2.498	2.490	27.7	26.4
expt[b]	2.472		26.8	

[a] The ECP used here is CRENBL, and the valence basis set used is aug-cc-pVnZ (n = D, T, Q, 5). [b] References 73 and 74.

2. Computational Details

In the present work, SO DFT calculations were performed employing the CRENBL[85,132−135] ECP, a spin-averaged relativistic effective potential (ARECP). The SO coupling effect is included using the two-component spinor formalism as proposed by Lee, Ermler, and Pitzer.[133] The ECP employed here treats the inner shell of gold (1s2s2p3s3p3d4s4p4d) as a core and treats the 19 valence electrons in the outer shell (5s5p5d6s) explicitly. Wang and Liu[136] suggested that a basis set containing a g function is sufficient for a four-component relativistic DFT calculation for gold. In the present work, a comparison between various basis sets is made to determine which basis set would be sufficient for a two-component relativistic DFT calculation of gold cluster. In Table 1, the bond lengths and the cohesive energy (atomization energy per atom) of Au_2 calculated by the SO BP86 and SO TPSSh methods employing the CRENBL ECP and the aug-cc-pVnZ (n = D, T, Q, 5) valence basis sets[94] (aug-cc-pVnZ/CRENBL) are presented.

From Table 1, it can be found that the bond length and cohesive energy of Au_2 are almost converged after aug-cc-pVQZ.[94] Enlarging the basis set shortens the bond length, while the cohesive energy increases at aug-cc-pVTZ, decreases at aug-cc-pVQZ, and then increases slightly at aug-cc-pV5Z. Both the bond length and the cohesive energy have a large change from aug-cc-pVDZ to aug-cc-pVTZ, and after aug-cc-pVTZ, the amplitude of variation becomes much smaller. The difference in bond length from aug-cc-pVTZ to aug-cc-pV5Z is just 0.003 Å for both functionals, while the difference in cohesive energy is just 0.5 kcal/mol for the SO BP86 method and 0.4 kcal/mol for the SO TPSSh method. These results indicate that in order to obtain accurate results for Au_2, a basis set larger than aug-cc-pVTZ is necessary. Unfortunately, SO DFT calculation using a basis set larger than aug-cc-pVTZ becomes very expensive. In Tables S1−S2 of the Supporting Information, we have listed the computational time for the SO TPSSh single-point energy calculations of Au_2 and Au_3 on a workstation with dual XEON E5506 CPU with all eight cores used for the parallel calculations. A single-point energy calculation of Au_3 at aug-cc-pVTZ took about 10 min, while at aug-cc-pVQZ, the time dramatically increased to more than 5 h. For geometry optimization, additional computational time is needed for the gradient calculation, which takes a much longer time than the single-point energy calculation for a basis set beyond aug-cc-pVTZ. Therefore, we have to choose the moderate aug-cc-pVTZ basis set based on a cost-effectiveness consideration, although the results at aug-cc-pVTZ have not been fully converged. This is a commonly adopted strategy for first-principle calculations since the accuracy of the calculation always depends on both the method and the basis set employed, and one has to make a compromise between accuracy and efficiency. In this sense, here, we are not evaluating the performance of a functional itself, that is, by using results at the complete basis set limit, but the performance of the combination of a functional with an incomplete basis set as a whole. In addition, Wang and Liu[136] concluded that including the g function is enough for a four-comonent relativity calculation of Au_2. Therefore, the aug-cc-pVTZ (11s10p9d3f2g)[94] valence basis set was used in the present work throughout. SC (SO-free) calculations were performed with the same valence basis set aug-cc-pVTZ (11s10p9d3f2g) and the same ARECP. All calculations were carried out with fine integral grid using the NWCHEM 5.1 software package.[83,84]

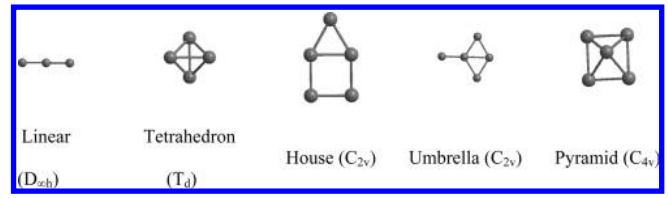

Figure 1. Transition-state structures optimized by the SO TPSS method.

Since the SO coupling effect depends on geometry, the geometries for gold clusters are fully optimized for each DFT method, with and without SO coupling. The SO correction to the atomization energy is defined as the difference between the atomization energy calculated by the SO DFT method and the DFT method without considering the SO coupling effect (SC DFT)

$$\Delta E_{SO} = [nE_{SO}(Au) - E_{SO}(Au_n)] - [nE_{SC}(Au) - E_{SC}(Au_n)] \quad (1)$$

where E_{SO} and E_{SC} are the potential energy calculated by the SO DFT method and the SC DFT method, respectively. In the present study, the cohesive energy (CE, kcal/mol) of a cluster is defined as the atomization energy per atom

$$CE = E_e(Au) - E_e(Au_n)/n \quad (2)$$

where E_e is the potential energy. To compare with experimental results, the zero-point vibrational energy (ZPE) contribution to the atomization energy or cohesive energy is removed from the experimental values quoted in the tables and text.

Starting geometries taken from the literature[10,18,89,91] were first optimized by employing the SO-free TPSS method (SC TPSS), followed by harmonic vibrational frequency analysis. Then, the optimized geometries were further refined by the SO DFT methods, and harmonic vibrational frequency was only performed using the SO TPSS method. The unstable structures (with imaginary vibrational frequencies) and stable local minimum structures (without imaginary vibrational frequencies) under the SO TPSS method are listed in Figures 1 and 2, respectively. A tight convergence criterion was used for geometry optimizations, and a default convergence criterion was used for SCF iterations.

3. Results and Discussion

3.1. Au_2. For Au_2, we have tried as many combinations of exchange and correlation functionals currently available in NWCHEM 5.1 as possible. A total of 240 combinations have

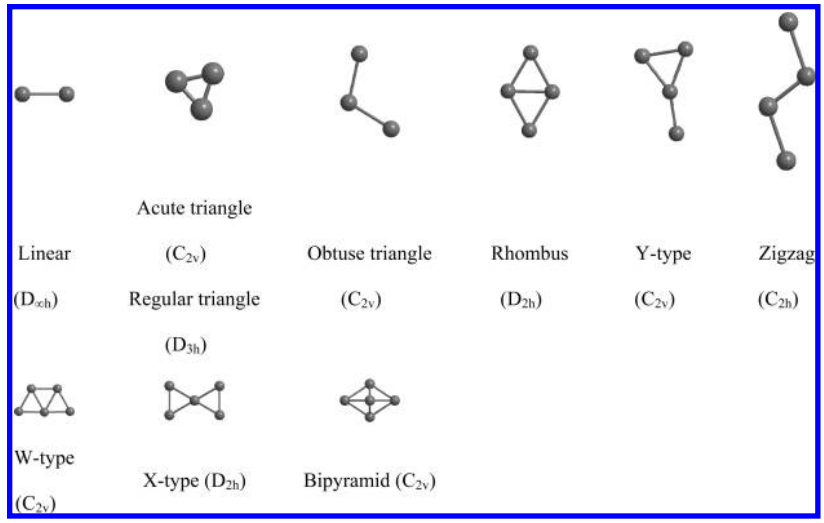

Figure 2. Local minimum structures without imaginary vibrational frequencies optimized by the SO TPSS method.

been tested. However, most of them do not show good performance. Only the results of the functionals with good performance (absolute error in cohesive energy not higher than 1.5 kcal/mol) and some popular functionals (for example B3LYP) are presented for discussion. The results of other functionals for Au_2 can be obtained from the Tables S5−S8 of the Supporting Information.

According to previous experimental studies, the accurate cohesive energy of Au_2 is 26.75 ± 0.05 kcal/mol.[73,74] Furthermore, previous theoretical studies indicate that spin−orbit coupling has a minor effect on Au_2.[137] The SO correction to the atomization energy (ΔE_{SO}) of Au_2 is just 0.6 kcal/mol according to recent work by Peterson and Puzzarini.[94] However, SO BP86 gives a cohesive energy of 27.6 kcal/mol when the result is converged, which is overestimated by almost 1 kcal/mol (Table 1). ΔE_{SO} calculated by SO BP86 is 3.0 kcal/mol. Other DFT functionals also give a similar ΔE_{SO} for Au_2 (Table 2). It was found that the cohesive energy calculated by the two-component relativistic BP86 method is higher than that calculated by the four-component relativistic BP86 method.[136] Therefore, the overestimation of the cohesive energy may be partly attributed to the overestimation of the two-component SO correction by the SO DFT method. Since the four-component relativistic BP86 method also overestimates the cohesive energy of Au_2 when the result is converged, the other cause of this overestimation may be the inaccuracy of the DFT functional itself.

According to Fabiano et al.,[138] inclusion of Hartree−Fock (HF) exchange into pure DFT functionals will underestimate the cohesive energy of the neutral and anionic Au_n ($n = 2-4$) clusters. This is in agreement with our results. By comparing results given by the M06-L, M06, M06-2X, and M06-HF series of functionals and the BLYP, B3LYP, BHandHLYP, and HFLYP series of functionals, it can be seen that the higher the proportion of the HF exchange, the lower the cohesive energy of Au_2 (Figure 3). From Figure 3, a linear relationship between the cohesive energy of Au_2 and the proportion of the HF exchange included in the functionals can be observed. A similar trend can also be observed for the PBE and PBEh and TPSS and TPSSh functionals (Table 2).

In the case of Au_2, the results given by the TPSSh, M06, B97-1, and B88PW91 functionals were very accurate when SO coupling was taken into consideration. This may be caused by the canceling effect of the overestimation effect of the SO coupling and the underestimation effect of the inclusion of the HF exchange to the cohesive energy. If no SO coupling is considered, PBE96, BP86, TPSS, and M06-L have good performance. If SO coupling is considered, the results given by the four functionals become worse because of the overestimation effect of SO coupling on the cohesive energy.

3.2. Au_3. Several isomers of the gold trimer have been investigated in the literature. One of them has a linear geometry (Figure 1), and the other two have a triangular geometry (Figure 2). However, in the present study, it was found that the linear structure ($D_{\infty h}$) is not a local minimum for the TPSS functional, whether SO coupling is considered or not. This does not agree with previous works.[22,139] For all of the DFT functionals, the linear structure always has the highest energy among the three possible isomers.

According to previous studies,[18,22,25] the triangular structure (C_{2v}) has two isomers (Figure 2). One is an obtuse triangle (Au_{3o}), and the other is an acute triangle (Au_{3a}). The lowering of symmetry from D_{3h} to C_{2v} is believed to be caused by the Jahn−Teller effect.[95] However, Rusakov et al.[86] pointed out that SO coupling plays an important role in the calculation of the relative energy (RE) and the geometries of the two isomers. When SO coupling is considered, the acute triangle structure will become the regular triangle (D_{3h}) one and is more stable than the obtuse triangle one. The RE between the two triangle isomers is 1.6 kcal/mol, calculated by the multireference AQCC method with SO correction calculated by the MPPT method.[86]

For the Au_3 cluster, the cohesive energies calculated by the same DFT functionals with good performance in the case of Au_2 are listed in Table 3. It can be seen from Table 3 that if no SO coupling is considered, Au_{3o} is predicted to be more stable than Au_{3a} by all of the pure DFT functionals except M06-L, by which the two isomers are almost degenerate in energy. On the other hand, some hybrid DFT functionals predict the obtuse triangle geometry to be more stable, while others predict the opposite. Generally, hybrid meta-GGA functionals perform better than hybrid GGA functionals on the relative stability of the two Au_3 isomers. Only 2 out of 10 hybrid GGA functionals, BHandH and MPW1K, correctly predict the right stability order. On the other hand, 7 out of 12 meta-GGA functionals correctly predict the right stability order.

When SO coupling is considered, more functionals give the right stability order for the two isomers. This indicates that the SO coupling effect in the Au_3 system is very important, and this is in agreement with the findings of Rusakov et al.[86] For all of the functionals, including SO coupling increases the

TABLE 2: Cohesive Energy (CE, kcal/mol) of Au_2 (kcal/mol)[a]

method	CE_{SC}	CE_{SO}	ΔE_{SO}
	GGA		
$B97^{GGA}$-1	25.1	26.6	2.9
BLYP	24.8	26.2	2.9
BOP	23.6	25.0	2.9
BP86	26.7	28.2	3.0
BPW91	25.5	26.9	3.0
FT97	28.8	30.2	2.8
HCTH	23.2	24.7	2.9
HCTH120	25.8	27.3	2.9
HCTH147	25.5	27.0	2.9
HCTH407	23.3	24.7	2.8
HCTH407P	23.2	24.6	2.7
HCTHP14	25.5	27.0	3.0
PBE96	26.9	28.4	3.0
PBEOP	24.6	26.0	2.9
PW91	27.1	28.6	3.0
	meta-GGA		
M06-L	27.1	28.5	2.8
PKZB99	24.8	26.3	3.0
TPSS	26.5	28.0	3.0
	hybrid GGA		
ACM	23.5	25.0	2.9
B3LYP	23.1	24.5	2.9
B97	24.5	25.9	2.9
B97-1	25.4	26.8	2.9
B97-2	24.9	26.3	2.9
B97-3	22.6	23.9	2.8
B98	25.0	26.4	2.9
BHandH	20.7	22.1	2.9
MPW1K	21.6	23.0	2.9
PBEh	23.9	25.4	2.9
	hybrid meta-GGA		
BB1K	22.7	24.1	2.9
M05	24.4	25.7	2.7
M05-2X	23.9	25.4	2.9
M06	25.7	27.1	2.8
M06-2X	18.2	19.6	2.8
M06-HF	13.5	15.2	3.5
MPW1B95	24.2	25.6	2.9
MPWB1K	22.9	24.4	2.9
PW6B95	24.1	25.5	2.9
PWB6K	22.6	24.1	2.9
TPSSh	25.3	26.8	2.9
VS98	28.1	29.5	2.8
expt.	26.6[b]	26.75 ± 0.05[c]	

[a] The subscripts SO and SC denote the results with SO coupling considered and without SO coupling considered, respectively. [b] Reference 145. [c] References 73 and 74.

atomization energy, but the atomization energy of Au_{3a} increases more than that of Au_{3o}. The atomization energy of Au_{3a} increases by 8.6 kcal/mol on average after including SO coupling, while that of Au_{3o} increases by 6.9 kcal/mol on average, 1.7 kcal/mol less than that of Au_{3a} (Table 4). Therefore, the inclusion of SO coupling increases the atomization energy of Au_{3a} more and thus stabilizes it more. In many cases, inclusion of SO coupling will make Au_{3a} the global minimum if it is not before including SO coupling. Therefore, for the SO DFT methods to correctly predict the right stability order, the RE of Au_{3o} to Au_{3a} without SO correction (RE_{SC}) should not be too negative. Thus, most pure GGA functionals except PBE96 and PW91, for which the two isomers are almost degenerate in energy, still give the wrong stability order since for these functionals, RE_{SC} is too negative (less than −2.2 kcal/mol). For the hybrid GGA functionals, now 4 out of 10 predict the right stability order. Others still predict

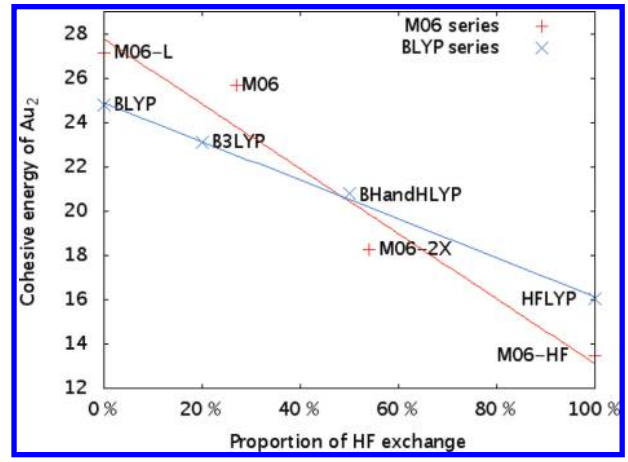

Figure 3. Cohesive energy of Au_2 calculated by the SC DFT functionals as a function of the proportion of HF exchange in the functional.

a wrong stability order since they give a RE_{SC} less than −2.5 kcal/mol, which is too negative. Meta-GGA and hybrid meta-GGA functionals perform better than GGA and hybrid GGA functionals. Two out of 3 meta-GGA functionals and 10 out of 12 hybrid meta-GGA functionals give the right stability order. Among all of the functionals predicting the right stability order, M06-L, PBEh, M06-HF TPSSh, and VS98 are the functionals that give the most accurate RE of 1.6 kcal/mol. Except for M06-L, the other four functionals are all hybrid functionals.

Similar to Au_2, hybrid DFT functionals also give a lower cohesive energy of Au_3 than the corresponding pure functionals, which agrees well with the results of Fabiano et al.[138] Probably owing to the canceling effect mentioned above, SO TPSSh performs the best on the cohesive energy of Au_3, followed by SO M06-L and SO M06. On the other hand, for the SO-free functionals, SC VS98 performs the best, followed by SC M06-L. However, SC VS98 overestimates the CE of Au_2 by 2.7 kcal/mol, which is not accurate enough in the building of reliable PESs. Except for its bad performance on CE of Au_2, SO VS98 is the best method among all of the SO and SO-free DFT methods in calculating RE. The RE calculated by SO VS98 is 1.6 kcal/mol, almost exactly the same value as that calculated by the accurate ab initio method.[86] The second and third best methods in calculating the RE of Au_3 are SO TPSSh and SO M06-L, respectively. SO PBEh and SO M06-HF also give very accurate RE for Au_3. However, considering their poor performances in the calculation of the cohesive energies of both Au_2 and Au_3, they were excluded in the study of the larger clusters Au_4 and Au_5. For Au_4 and Au_5, SO DFT calculations become very expensive. Therefore, among the 40 functionals, for only those functionals performing well for Au_3, that is, BP86, M06-L, PBE96, PBEh, PKZB99PWB6k (Table S9 in the Supporting Information), TPSS, TPSSh, and VS98, and the popular B3LYP functional, a total of nine functionals are employed to calculate Au_4 and Au_5.

3.3. Au_4. For Au_4, the rhombus (Au_{4R}), Y-type (Au_{4Y}), zigzag (Au_{4Z}), and tetrahedron (Au_{4T}) structures as shown in Figures 1 and 2 have been studied. Harmonic vibrational analysis indicates that the highly symmetrical tetrahedron structure is not a local minimum, whether SO coupling is considered or not. Some previous studies reported the tetrahedron structure as a possible isomer of Au_4.[18,22] We have repeated the calculations using the PW91PW91/LANL2DZ method without SO coupling (Table S10 of the Supporting Information). If no symmetry constraint is applied, PW91PW91/LANL2DZ would

TABLE 3: Cohesive Energy (CE kcal/mol per atom) and Relative Energy (RE, kcal/Mol) of the Two Isomers of Au_3[a]

	Au_{3a}		Au_{3o}			
	CE_{SC}	CE_{SO}	CE_{SC}	CE_{SO}	RE_{SC}	RE_{SO}
			GGA			
$B97^{GGA}$-1	22.9	25.8	24.7	27.0	−5.2	−3.5
BLYP	23.8	26.9	25.3	27.9	−4.7	−2.9
BOP	22.0	24.9	23.7	26.1	−5.1	−3.5
BP86	27.0	30.2	27.9	30.5	−2.7	−0.7
BPW91	25.4	28.6	26.3	28.9	−2.7	−0.8
FT97	28.2	31.4	29.1	31.7	−2.8	−0.8
HCTH[b]	NA	23.8	22.7	25.1	NA	−3.7
HCTH120	24.3	27.2	25.9	28.2	−4.9	−3.0
HCTH147	23.9	26.9	25.5	27.9	−4.9	−3.0
HCTH407[b]	NA	24.2	23.1	25.3	NA	−3.4
HCTH407P[b]	NA	23.7	22.9	25.0	NA	−4.0
HCTHP14	25.8	28.9	26.6	29.0	−2.4	−0.3
PBE96	27.4	30.6	28.1	30.6	−2.2	0.0
PBEOP	23.4	26.5	25.0	27.5	−4.7	−3.0
PW91	27.7	31.0	28.4	31.0	−2.1	0.0
			meta-GGA			
M06-L	27.7	30.5	27.7	29.9	0.0	1.7
PKZB99	24.8	27.9	25.5	28.0	−2.2	−0.4
TPSS	27.4	30.5	27.7	30.2	−1.0	0.9
			hybrid GGA			
ACM	23.2	26.0	23.6	25.9	−1.2	0.6
B3LYP	22.0	24.8	23.0	25.2	−2.9	−1.0
B97	23.3	26.1	24.2	26.4	−2.8	−1.0
B97-1	24.4	27.3	25.2	27.5	−2.5	−0.6
B97-2	23.4	26.2	24.3	26.5	−2.7	−0.9
B97-3	21.0	23.5	21.8	23.9	−2.6	−1.2
B98	23.9	26.7	24.7	27.0	−2.6	−0.8
BHandH	20.6	23.2	20.5	22.6	0.4	1.8
MPW1K	21.4	24.1	21.2	23.4	0.6	2.1
PBEh	24.0	26.8	24.1	26.3	−0.2	1.6
			hybrid meta-GGA			
BB1K	22.6	25.4	22.1	24.3	1.5	3.3
M05	22.9	25.6	23.3	25.3	−1.1	0.9
M05-2X	23.0	25.2	23.5	25.6	−1.6	−1.3
M06	25.6	28.4	25.5	27.6	0.1	2.5
M06-2X	17.7	20.1	18.2	20.1	−1.6	−0.2
M06-HF	14.4	17.3	14.3	16.7	0.5	1.7
MPW1B95	24.3	27.2	24.0	26.2	0.9	3.1
MPWB1K	23.0	25.8	22.5	24.6	1.7	3.5
PW6B95	24.0	26.9	23.9	26.1	0.2	2.4
PWB6K	22.6	25.3	22.1	24.2	1.5	3.3
TPSSh	25.9	28.9	26.0	28.3	−0.3	1.7
VS98	28.5	31.4	28.6	30.9	−0.3	1.6
expt	29.2 ± 1.0[c]					1.6[d]

[a] Au_{3a} and Au_{3o} represent the acute triangle and the obtuse triangle geometry of Au_3, respectively. The subscripts SO and SC denote the results with SO coupling considered and without SO coupling considered, respectively. If SO coupling is considered, the optimized geometry of Au_3 is a regular triangle (D_{3h}). The relative energy (RE) is defined as $E_{Au3o} - E_{Au3a}$. [b] These functionals do not give stable acute triangle geometries of Au_3 if no SO coupling is considered. [c] Reference 75. [d] MR AQCC result with SO correction calculated by the MPPT method.[86]

give a slightly distorted tetrahedron structure starting from a tetrahedron structure. Its atomization energy is higher than that of Au_{4R} by 32.2 kcal/mol. If the structure is forced to keep the T_d symmetry during geometry optimization, the energy of the optimized tetrahedron structure is higher than that of Au_{4R} by 36.7 kcal/mol. Similar to Au_3, this distortion should be caused by the Jahn−Teller effect. If SO coupling is considered and no symmetry constraint is applied, a tetrahedron can be optimized by PW91PW91 with the cc-pVDZ/CRENBL basis set (it should be noted that the LANL2DZ basis set is terrifically bad for SO DFT calculations), and its energy is higher than that of Au_{4R} by 25.0 kcal/mol. Similar to the PW91PW91 functional, by using the TPSS functional with the LANL2DZ basis set, without SO coupling, a distorted tetrahedron structure can be optimized, while with SO coupling, the optimized structure becomes a tetrahedron. However, SO TPSS with a larger aug-cc-pVTZ/CRENBL basis set does not give a tetrahedron structure if no symmetry constraint is applied. The tetrahedron structure is not a local minimum, and the optimization ends up with the rhombus structure (Au_{4R}). If symmetry constraint is applied, the energy of the optimized tetrahedron Au_4 is higher than that of Au_{4R} by 23.4 kcal/mol. Therefore, it seems that small basis sets such as the LANL2DZ and cc-pVDZ/CRENBL basis sets are not good enough for the calculation of the Au_4 cluster.

Some previous studies[11,18,22] have reported that the global minimum structure of the neutral gold clusters from Au_4 to Au_n ($n = 7-15$) are all planar. In the present work, the planar rhombus structure is found to be the global minimum for all of the DFT methods if SO coupling is considered, which agrees with previous work. However, the relative energies between the

TABLE 4: SO Correction (ΔE_{SO}, kcal/mol) to the Atomization Energy of Au_3[a]

method	ΔE_{SOa}	ΔE_{SOo}
GGA		
$B97^{GGA}$-1	8.8	7.0
BLYP	9.3	7.6
BOP	9.0	7.4
BP86	9.8	7.8
BPW91	9.5	7.6
FT97	9.9	7.9
HCTH	3.2	6.9
HCTH120	8.8	7.0
HCTH147	8.9	7.1
HCTH407	3.2	6.6
HCTH407P	2.4	6.4
HCTHP14	9.4	7.3
PBE96	9.8	7.7
PBEOP	9.2	7.4
PW91	9.8	7.7
meta-GGA		
M06-L	8.3	6.6
PKZB99	9.4	7.6
TPSS	9.4	7.5
hybrid GGA		
ACM	8.6	6.8
B3LYP	8.4	6.6
B97	8.4	6.7
B97−1	8.5	6.7
B97−2	8.3	6.5
B97−3	7.7	6.2
B98	8.5	6.7
BHandH	7.7	6.3
MPW1K	7.9	6.4
PBEh	8.5	6.7
hybrid meta-GGA		
BB1K	8.2	6.4
M05	7.9	5.9
M05-2X	6.7	6.4
M06	8.5	6.2
M06-2X	7.2	5.8
M06-HF	8.5	7.3
MPW1B95	8.8	6.6
MPWB1K	8.2	6.4
PW6B95	8.8	6.6
PWB6K	8.1	6.3
TPSSh	9.0	7.1
VS98	8.7	6.8
average	8.6[b]	6.9

[a] The subscripts a and o denote the acute triangle Au_3 and obtuse triangle Au_3, respectively. [b] Average value excluding the values calculated by the HCTH, HCTH407, and HCTH407P functionals.

isomers reported here are very different from those in the literature. For example, the Y-type structure is just 0.3 kcal/mol higher in energy than the rhombus structure calculated by the SC PW91PW91/LANL2DZ method[91] and is 1.8 kcal/mol higher in energy calculated by the SC PW91PW91/CRENBL method,[22] while in the present study, it is 3.0 kcal/mol higher in energy calculated by the SO TPSSh method (Table 5), a method which has shown very good performance in the calculation of the RE of the two Au_3 isomers and the atomization energy of both Au_2 and Au_3. The RE between the zigzag structure and the rhombus structure is calculated to be 10.9 kcal/mol by the PW91PW91/CRENBL method,[22] which is close to the values calculated by the SC TPSS, SC TPSSh, and SC PBEh methods but smaller than the value calculated by the SO TPSSh method. It should be noted that BP86 and B3LYP will give a wrong stability order when SO coupling is not considered (Table 6). For SC B3LYP, the Y-type structure is lower in energy than the rhombus structure by 1.6 kcal/mol, while for SC BP86, the two structures almost have the same energy.

TABLE 5: SO-Corrected Cohesive Energies (CE, kcal/mol) and Relative Energies (RE, kcal/mol) of the Three Isomers of Au_4[a]

	CE_{SO}			RE_{SO}		
	Au_{4R}	Au_{4Y}	Au_{4Z}	Au_{4R}	Au_{4Y}	Au_{4Z}
B3LYP	32.2	32.2	30.0	0.0	0.2	8.9
BP86	38.5	38.0	35.5	0.0	2.1	11.8
M06-L	39.3	38.4	35.3	0.0	3.7	15.9
PBE96	39.0	38.4	35.8	0.0	2.6	12.7
PBEh	34.9	34.4	31.4	0.0	2.2	14.1
PKZB99PWB6k	38.0	37.1	34.1	0.0	3.7	15.6
TPSS	39.1	38.3	35.4	0.0	3.2	14.7
TPSSh	37.3	36.5	33.5	0.0	3.0	15.1
VS98	40.3	39.1	36.2	0.0	4.6	16.2

[a] Relative energy is defined as the relative energy between an isomer and the global minimum structure. The subscript R is for the rhombus structure, Y for the Y-type structure, and Z for the zigzag structure.

TABLE 6: SC Cohesive Energies (CE, kcal/mol) and Relative Energies (RE, kcal/mol) of the Three Isomers of Au_4[a]

	CE_{SC}			RE_{SC}		
	Au_{4R}	Au_{4Y}	Au_{4Z}	Au_{4R}	Au_{4Y}	Au_{4Z}
B3LYP	29.0	29.4	27.5	1.6	0.0	7.3
BP86	34.9	35.0	32.9	0.1	0.0	8.3
M06-L	36.1	35.6	32.9	0.0	1.8	12.6
PBE96	35.5	35.4	33.2	0.0	0.4	9.1
PBEh	31.6	31.5	28.9	0.0	0.4	10.9
PKZB99PWB6k	34.5	34.1	31.5	0.0	1.5	11.9
TPSS	35.6	35.3	32.8	0.0	1.0	11.1
TPSSh	33.9	33.6	31.0	0.0	1.0	11.6
VS98	37.0	36.3	33.8	0.0	2.8	12.9
CCSD(T)	36.2 (36.4)[b]	35.5[c]	31.9[c]	0.0	2.9	17.3

[a] Relative energy is defined as the relative energy between an isomer and the global minimum structure. The subscript R is for the rhombus structure, Y for the Y-type structure, and Z for the zigzag structure. [b] The value in the parentheses is calculated by extrapolating energies to complete basis set limit (see text for the details on the extrapolation). [c] Calculated using single-point energies at the CCSD(T)/aug-cc-pVTZ level on the SO TPSSh geometries.

For the Au_4 cluster, there is no experimental cohesive energy available. To determine which SC DFT method is better, the rhombus geometry of Au_4 was optimized at the CCSD(T) level by a numerical method. The PES of the rhombus geometry of Au_4 was first scanned at the CCSD(T) level with the aug-cc-pVTZ/CRENBL basis set by varying the a and b geometry parameters of the rhombus structure, as shown in Figure 4. The resulting PES is shown in Figure 5. The PES was then fitted via the following quadratic function

$$E(a,b) = c_1a^2 + c_2b + c_3b^2 + c_4b + c_5ab + c_6 \quad (3)$$

where c_1-c_6 are fitting parameters. The fitted parameters are $c_1 = 0.384201$, $c_2 = -2.40887$, $c_3 = 0.704643$, $c_4 = -2.95551$, $c_5 = 0.489247$, and $c_6 = -537.986$. The root-mean square (rms) of residuals is 2.97×10^{-8}, which indicates that the fitting is very accurate. The global minimum structure is located at (2.310, 1.295), as shown in Figure 5. Then, single-point energies of this global minimum structure are performed at the MP2 level

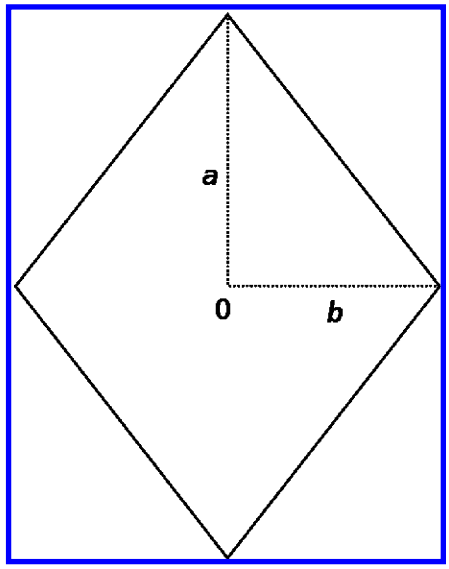

Figure 4. The scheme used to scan the potential energy surface of the rhombus structure of Au_4, in which *a* and *b* geometry parameters were varied.

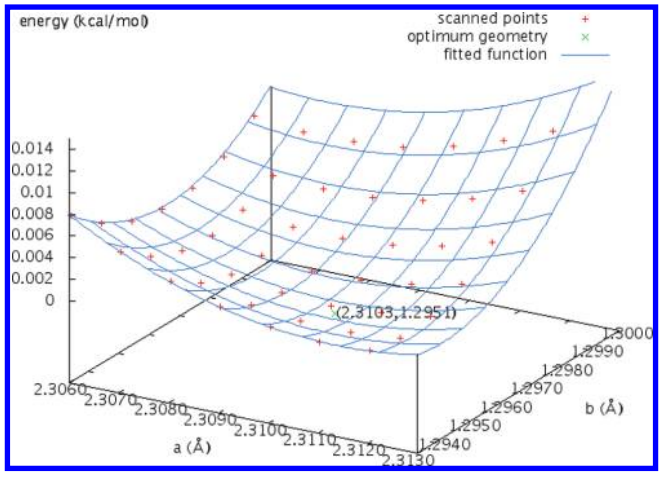

Figure 5. The potential energy surface of the rhombus structure of Au_4.

with the aug-cc-pVDZ, aug-cc-pVTZ, and aug-cc-pVQZ valence basis sets and the CRENBL ECP. The three MP2 energies are then extrapolated to the complete basis set limit (CBS) employing eq 4[140,141]

$$E_x = E_{\mathrm{CBS}} + A \cdot \mathrm{e}^{Bx} \quad (4)$$

The CCSD(T)/CBS energy is estimated by the following eq 5

$$E_{\mathrm{CCSD(T)/CBS}} \approx E_{\mathrm{CCSD(T)/aug\text{-}cc\text{-}pVTZ}} + (E_{\mathrm{MP2/CBS}} - E_{\mathrm{MP2/aug\text{-}cc\text{-}pVTZ}}) \quad (5)$$

The accurate cohesive energy of rhombus Au_4 at the CCSD(T)/CBS level is then estimated to be 36.4 kcal/mol. In comparison, the cohesive energy at the CCSD(T)/aug-cc-pVTZ level is 36.2 kcal/mol, indicating that the aug-cc-pVTZ basis set is large enough for the calculation of the cohesive energy of Au_4. For the Y-type and zigzag structures of Au_4, at the CCSD(T) level, only single-point energy calculations are performed with the aug-cc-pVTZ valence basis set using the geometries optimized by the SO TPSSh method.

From Table 6, it can be seen that the cohesive energy of rhombus Au_4 given by SC M06-L (36.1 kcal/mol) is the closest one to that by CCSD(T)/CBS. SC VS98 is the second one, followed by SC TPSS and SC PBE96. However, SC M06-L, SC PBE96, and SC TPSS all greatly underestimate the relative energies of the Y-type and the zigzag structure for the rhombus structure. SC VS98, on the other hand, gives almost the same RE of the Y-type structure as CCSD(T) while greatly underestimating the RE of the zigzag structure as do all of the other SC DFT methods.

For the SO DFT methods, the cohesive energy of the rhombus Au_4 given by SO TPSSh is 37.3 kcal/mol. Except for SO B3LYP and SO PBEh, all other methods give higher cohesive energies than SO TPSSh. However, since no accurate cohesive energy calculated at the CCSD(T) level with SO correction is available, and considering the good performance of SO TPSSh in the cases of both Au_2 and Au_3, it should be reasonable to assume that the cohesive energy calculated by the SO TPSSh method is accurate. Compared to the SO TPSSh results, the results from SC VS98 are the closest, followed by those from SC M06-L and SC TPSS. The best cohesive energy calculated here is higher than the literature values, the 30.8 kcal/mol[89] calculated by the SC B3PW91/LANL2DZ method, and the 33.5 kcal/mol calculated by the SC PW91PW91/LANL2DZ method.[91] The lower cohesive energies given by the previous studies may be caused by neglect of the SO coupling effect, the incompleteness of the basis set, and the inaccuracy of the functionals as well.

From Tables 5 and 6, it can be seen that including SO correction greatly increases the cohesive energy of Au_4, as in the cases of Au_2 and Au_3. If CCSD(T)/CBS is the method that gives the most accurate SC results, while SO TPSSh gives the most accurate SO results, it can be seen that the SO correction given by the SO DFT methods may be overestimated. The difference between the cohesive energies calculated by the CCSD(T)/CBS method and the SO TPSSh method is not so large compared to the cohesive energy difference calculated by the SC TPSSh method and the SO TPSSh method. On the other hand, the relative energies given by the SO DFT methods are much closer to the values given by the SC CCSD(T) method than those given by the SC DFT methods. Comparing results in Tables 5 and 6 indicates that SO coupling has a very large effect on the relative energies of the Au_4 cluster calculated by the DFT methods.

3.4. Au_5. In the case of Au_5, only three stable structures were found, two 2D structures, the W-type (Au_{5W}) and the X-type (Au_{5X}) structures, and one 3D structure, the bipyramid (Au_{5B}) structure. The two structures with the C_{4v} and C_{2v} symmetry (Figure 1) are transition-state structures with imaginary vibrational frequencies. Among the three local minimum structures, the most stable one is Au_{5W}, in agreement with previous works.[10,18,89,91] According to Walker,[22] the order of the stability for the three isomers of Au_5 is $Au_{5W} > Au_{5X} > Au_{5B}$, calculated by SC PW91PW91. In the present study, it was found that when SO coupling is not considered, all nine methods also give the same stability order as SC PW91PW91 (Table 7). However, different methods may give very different relative energies. For Au_{5X}, its RE to the Au_{5W} is calculated to be between 7.8 and 12.5 kcal/mol, while for Au_{5B}, its RE is calculated to be between 12.7 and 24.3 kcal/mol. A much higher RE of the Au_{5B} to Au_{5W} has been reported in the literature; for example, Li et al. have reported this RE to be 31.8 kcal/mol, which is calculated by the SC PW91PW91/LANL2DZ method.[91] It should be noted that by using the same method, Walker has obtained a much lower RE for Au_{5B}, which is just 18.9 kcal/mol.

TABLE 7: SC Cohesive Energies (CE, kcal/mol) and Relative Energies (RE, kcal/mol) of the Three Isomers of Au_5[a]

	CE_{SC}			RE_{SC}		
	Au_{5W}	Au_{5X}	Au_{5B}	Au_{5W}	Au_{5X}	Au_{5B}
TPSS	39.1	37.2	35.2	0.0	9.9	19.9
VS98	40.4	37.9	37.9	0.0	12.5	12.7
PBEh	35.0	33.1	30.6	0.0	9.5	21.9
TPSSh	37.4	35.4	33.4	0.0	10.0	20.3
M06-L	39.5	37.3	36.4	0.0	11.0	15.5
BP86	38.3	36.5	33.8	0.0	9.1	22.4
PKZB99PWB6k	37.8	35.7	34.6	0.0	10.4	15.8
PBE96	38.9	37.0	34.6	0.0	9.2	21.4
B3LYP	31.9	30.3	27.0	0.0	7.8	24.3

[a] Relative energy is defined as the relative energy between an isomer and the global minimum structure. The subscript W is for the W-type structure, X for the X-type structure, and B for the bipyramid structure.

TABLE 8: SO-Corrected Cohesive Energies (CE, kcal/mol) and Relative Energies (RE, kcal/mol) of the Three Isomers of Au_5[a]

	CE_{SO}			RE_{SO}		
	Au_{5W}	Au_{5X}	Au_{5B}	Au_{5W}	Au_{5X}	Au_{5B}
TPSS	42.9	40.6	40.0	0.0	11.4	14.3
VS98	43.9	41.1	42.4	0.0	13.7	7.5
PBEh	38.5	36.4	35.1	0.0	10.6	17.0
TPSSh	41.1	38.8	38.1	0.0	11.3	15.0
M06-L	43.0	40.5	40.9	0.0	12.2	10.3
BP86	42.1	39.9	38.7	0.0	10.6	16.9
PKZB99PWB6k	41.6	39.2	39.6	0.0	12.0	9.9
PBE96	42.6	40.5	39.4	0.0	10.8	15.9
B3LYP	35.4	33.6	31.4	0.0	9.0	19.7

[a] Relative energy is defined as the relative energy between an isomer and the global minimum structure. The subscript W is for the W-type structure, X for the X-type structure, and B for the bipyramid structure.

Similar to the Au_2-Au_4 clusters, including SO correction greatly increases the cohesive energy of the Al_5 cluster. Among all nine SO DFT methods, the cohesive energy of the global minimum (Au_{5W}) calculated by PKZB99PWB6k (41.6 kcal/mol) is closest to the one calculated by SO TPSSh (41.1 kcal/mol)(Table 8). For those SC DFT methods, VS98 gives the closest cohesive energy (40.1 kcal/mol), followed by M06-L (39.5 kcal/mol) and TPSS (39.1 kcal/mol). SO coupling also has a significant effect on the calculation of relative energies. It increases the RE between Au_{5X} and Au_{5W} by 1.1−1.6 kcal/mol. On the other hand, it decreases the RE between the 3D structure (Au_{5B}) and Au_{5W} by 4.6−5.9 kcal/mol. After including SO correction, for the VS98, M06-L, and PKZB99PWB6k methods, the 3D structure is even more stable than Au_{5X}. Taking the performance on both cohesive energy and RE into consideration, SO BP86 is the SO DFT method, while SC M06-L is the SC DFT method that gives closest results to the SO TPSSh method.

4. Discussion

4.1. Best Results for the Au_2-Au_5 Clusters. In the previous section, we have shown that SC M06-L can give similar results to SC CCSD(T) while SO TPSSh gives the closest results to experiment for Au_2 and Au_3. In Table 9, we have summarized the results for the Au_2-Au_5 clusters calculated by the SC CCSD(T), SC M06-L, and SO TPSSh methods employing the aug-cc-pVTZ/CRENBL basis set. For the Au_5 cluster, the calculation at the CCSD(T) level using the aug-cc-pVTZ valence basis set is very expensive and was not performed. From the table, it can be seen that due to the absence of SO correction, the cohesive energy of Au_3 calculated by the CCSD(T) method is not very accurate. However, it correctly predicts that acute triangle Au_3 is more stable than obtuse triangle Au_3 even when no SO coupling is considered. It seems that SO correction is important for the DFT method to predict correct stability order for the two isomers of Au_3 but not for the CCSD(T) method. M06-L has similar performance as CCSD(T) on the cohesive energies of Au_2 and Au_4 and the relative energies of the three Au_4 isomers. However, it predicts that the two isomers of Au_3 are almost degenerate in energy. SO TPSSh performs best on both the cohesive energies of Au_2-Au_3 and the RE between the two isomers of Au_3. There is no reason that we should not trust this method for the calculation of Au_4, Au_5, and even larger gold clusters. SC M06-L performs relatively well, and it can give quantitatively and qualitatively similar results to SO TPSSh, except the RE of the two isomers of Au_3. Therefore, considering that SO DFT calculations are expensive, M06-L is also a good candidate for the study of large gold clusters. Recently, Truhlar et al. have studied the 2D−3D transition of the ions of the gold clusters, and they found that the 2D−3D transition point predicted by the SC M06-L method is in good agreement with experimental results.[142] Similar work has also been done by Ferrighi et al., who also show that SC M06-L exhibits good performance in 2D−3D transition.[143]

TABLE 9: Best Cohesive Energies (kcal/mol) of Au_2-Au_5 from DFT Methods and the CCSD(T) Method[a]

	CCSD(T)	SC M06-L	SO TPSSh	expt
Au_2	26.7	27.1	26.8	26.8[b]
Au_{3a}	27.0	27.7	28.9	29.2[c]
Au_{3o}	26.1	27.7	28.3	28.7[d]
Au_{4R}	36.2	36.1	37.3	NA
Au_{4Y}	35.5[e]	35.6	36.5	NA
Au_{4Z}[c]	32.0[e]	32.9	33.5	NA
Au_{5W}	NA	39.5	41.1	NA
Au_{5X}	NA	37.3	38.8	NA
Au_{5B}	NA	36.4	38.1	NA

[a] The valence basis set used here is aug-cc-pVTZ, and the ECP is CRENBL. [b] References 73 and 74. [c] Reference 75. [d] The cohesive energy of obtuse triangle Au_3 is calculated by the MR AQCC method with SO correction.[86] [e] The geometries of Au_{4Y} and Au_{4Z} are optimized by the SO TPSS method.

TABLE 10: Average Cohesive Energies (ACE, kcal/mol), Mean Errors (ME, kcal/mol), and Mean Absolute Errors (MAE, kcal/mol) of Various Types of DFT Functionals

functional category	ACE_{SC}	ACE_{SO}	ME_{SC}	ME_{SO}	MAE_{SC}	MAE_{SO}
			Au_2			
GGA	25.3	26.8	−1.4	0.0	1.4	1.3
meta-GGA	26.1	27.6	−0.6	0.9	0.9	1.2
hybrid GGA	23.5	25.0	−3.2	−1.8	3.2	1.8
hybrid meta-GGA	23.0	24.4	−3.8	−2.3	4.0	2.9
			Au_{3a}			
GGA	24.7	27.4	−4.5	−1.8	4.1	2.7
meta-GGA	26.6	29.6	−2.6	0.4	2.6	1.3
hybrid GGA	22.7	25.5	−6.5	−3.7	6.5	3.7
hybrid meta-GGA	22.9	25.6	−6.3	−3.6	6.3	3.9

4.2. Performance of Different Types of Functionals. In Table 10, the average performance of different types of functionals on the cohesive energy of Au_2 and the acute triangle Au_3, for which accurate experimental results are available, has been summarized. It can be seen that SC GGA functionals do give poorer results than SC meta-GGA functionals. In the case

of Au_2, the mean absolute error (MAE) of SC GGA functionals is 1.4 kcal/mol, while that of SC meta-GGA functionals is 0.9 kcal/mol. SC GGA functionals systematically underestimate the cohesive energy of Au_2 with a mean error (ME) of −1.4 kcal/mol. For the larger cluster Au_3, such a trend becomes more obvious; the MAE of SC GGA functionals is 4.1 kcal/mol, while that of SC meta-GGA functionals is 2.6 kcal/mol. The cohesive energy of Au_3 is also systematically underestimated by most SC GGA and SC meta-GGA functionals.

Meta-GGA functionals also perform better than GGA functionals with SO coupling considered. The MAE of SO GGA functionals is 1.3 kcal/mol for Au_2 and 2.7 kcal/mol for Au_3. On the other hand, the MAE of SO meta-GGA functionals is 1.2 kcal/mol for Au_2 and 1.3 kcal/mol for Au_3. Furthermore, SO meta-GGA functionals perform better than SO GGA DFT functionals on the RE of the two isomers of Au_3; 13 out of 15 SO GGA functionals prefer obtuse triangle Au_3, and the rest two give a result that the two isomers are almost degenerate in energy, as shown in Table 3. On the other hand two out of three SO meta-GGA functionals prefer acute triangle Au_3, and PKZB99 gives the wrong stability order.

Inclusion of HF exchange systematically underestimates the cohesive energy of both Au_2 and Au_3 compared to the pure functionals. The extent of such underestimation is very similar for the hybrid GGA and hybrid meta-GGA functionals. On average, SC hybrid GGA functionals underestimate the cohesive energy of Au_2 by 3.2 kcal/mol and Au_3 by 6.5 kcal/mol, while SC hybrid meta-GGA functionals underestimate the cohesive energy of Au_2 by 3.8 kcal/mol and that of Au_3 by 6.3 kcal/mol. The same trend can also be observed after SO coupling is considered; SO hybrid GGA functionals systematically underestimates the cohesive energy of Au_2 and Au_3 by 1.8 and 3.7 kcal/mol, respectively, while SO hybrid meta-GGA functionals underestimate the energy by 2.3 and 3.6 kcal/mol, respectively. Unlike pure functionals, after inclusion of HF exchange, the performance of meta-GGA functionals on the cohesive energies of Au_2 and Au_3 is generally worse than that of GGA functionals, with the exception that SC meta-GGA functionals perform slightly better than SC GGA functionals on Au_3.

On the other hand, SO hybrid meta-GGA functionals perform better than SO hybrid GGA functionals on the RE of the two isomers of Au_3. As discussed above, only 4 out of 10 SO hybrid GGA functionals give the right stability order, while 10 out of 12 SO hybrid meta-GGA functionals give the right stability order. The average RE calculated by the meta-GGA functionals giving the right stability order is 2.4 kcal/mol. In comparison, the corresponding value calculated by the GGA functionals is 1.5 kcal/mol.

4.3. Effect of SO Coupling. SO correction to the atomization energy (ΔE_{SO}) of Au_2 is almost functional-independent, as shown in Table 2. For most functionals, the correction falls in a narrow range between 2.8 and 3.0 kcal/mol. The largest correction, 3.5 kcal/mol, is given by the M06-HF functional, while the smallest value, 2.7 kcal/mol, is given by the HCTH407P and M05 functionals. However, ΔE_{SO} of Au_3 varies in a much larger range, as shown in Table 4. Except the atomization energy of Au_{3a} calculated by the HCTH, HCTH407, and HCTH407P functionals, ΔE_{SO} of Au_{3a} falls in a range between 6.7 and 9.9 kcal/mol, while that of Au_{3o} falls in a narrower range between 5.8 and 7.9 kcal/mol. Excluding the three functionals of the HCTH family, the average ΔE_{SO} of Au_{3a} is 8.6 kcal/mol, while that of Au_{3o} is lower, 6.9 kcal/mol (average over all values).

TABLE 11: SO Correction (kcal/mol) to the Atomization Energy of Au_4 and Au_5[a]

	Au_{4R}	Au_{4Y}	Au_{4Z}	Au_{5W}	Au_{5X}	Au_{5B}
B3LYP	12.9	11.2	9.8	17.4	16.3	22.1
BP86	14.2	12.0	10.6	18.8	17.3	24.3
M06-L	12.9	11.1	9.6	17.3	16.1	22.6
PBE96	14.1	11.9	10.5	18.8	17.2	24.3
PBEh	13.2	11.4	10.0	17.8	16.7	22.7
PKZB99PWB6k	14.2	12.0	10.5	18.9	17.3	24.9
TPSS	14.0	11.9	10.4	18.6	17.2	24.2
TPSSh	13.6	11.6	10.2	18.2	16.9	23.5
VS98	12.9	11.1	9.6	17.2	16.0	22.4

[a] The subscript R is for the rhombus structure, Y for the Y-type structure, Z for the zigzag structure, W for the W-type structure, X for the X-type structure, and B for the bipyramid structure.

TABLE 12: SO Correction (kcal/mol) to the Atomization Energy Calculated by SO TPSS for Small Gold Clusters

	N_{atom}[a]	N_{bond}[b]	ΔE_{SO}	ΔE_{SO} fitted	residual error
Au_2	2	1	3.0	3.7	−0.8
Au_{3a}	3	3	9.4	9.0	0.5
Au_{3o}	3	2	7.5	6.7	0.8
Au_{4R}	4	5	14.0	14.2	−0.2
Au_{4Y}	4	4	11.9	11.9	−0.1
Au_{4Z}	4	3	10.4	9.7	0.8
Au_{5W}	5	7	18.6	19.5	−0.8
Au_{5X}	5	6	17.2	17.2	0.0
Au_{5B}	5	9	24.2	24.0	0.2

[a] N_{atom} is the number of gold atoms. [b] N_{bond} is the number of bonds between gold atoms.

ΔE_{SO} of Au_4 and Au_5 are collected in Table 11. The results indicate that all nine DFT functionals employed here give a very similar ΔE_{SO} for the same isomer with the same cluster size. For example, in the case of Au_{4R} (the rhombus Au_4), the maximum ΔE_{SO} is 14.2 kcal/mol, and the minimum is 12.9 kcal/mol, with a range of just 1.3 kcal/mol. This trend is similar to that found for Au_2 and Au_3. A conclusion that can be drawn is that the ΔE_{SO} of small gold clusters depends weakly on the functionals employed. This finding may be helpful in calculating ΔE_{SO} of larger gold cluster since simpler functionals instead of complex functionals could be employed to calculate SO corrections.

From Tables 4 and 11, it can be seen that different isomers of a cluster have different ΔE_{SO} values. To rationalize the trend in the SO corrections, we have analyzed the data and tried to build an empirical relationship between ΔE_{SO} and the number of gold atoms and gold−gold bonds in the clusters. The following simple linear equation has been tried:

$$\Delta E_{SO} = aN_{atom} + bN_{bond} \quad (6)$$

where N_{atom} is the number of gold atoms and N_{bond} is the number of Au−Au bonds in the cluster. To judge if two gold atoms are bonded, the criterion used by the popular visualization software MOLDEN 4.7[144] is employed where two gold atoms having a distance shorter than 3.4 Å are bonded. Since the dependence of ΔE_{SO} on the functionals is weak except for a few functionals, we have only fitted the ΔE_{SO} values calculated by the TPSS functional with eq 6. Using $1/\Delta E_{SO}$ as the weight, the weighted least-squares fitting gives $a = 0.718$ and $b = 2.27$. The weighted residual sum of squares is just 0.40, indicating that the fitting is very good. The fitting data and the fitted results are presented in Table 12. From the table, it can be seen that the residual error for each structure is very small.

This equation may be used as a rule of thumb to estimate ΔE_{SO} of the gold clusters not calculated in the present study. From the equation, it can be seen that ΔE_{SO} does not simply depend on the number of gold atoms, which agrees with the fact that ΔE_{SO} values of different isomers of the same cluster size are significantly different. In fact, ΔE_{SO} depends linearly on both the number of gold atoms and Au−Au bonds in the cluster. Given the same cluster size, that is, the same N_{atom}, according to eq 6, the structures with more bonds have higher ΔE_{SO} and thus become more stable. Generally, 3D structures have more bonds than 2D structures of the same cluster size. If the equation is applicable to other clusters as well (our preliminary calculations indicate that this relationship can also be applied to Au_6), it can be deduced that inclusion of SO correction will favor the 3D structures of the gold clusters. Thus, SO coupling may play an important role in the 2D−3D transition of gold clusters if DFT methods are used. Previous studies[142,143] have found that both the SC TPSS and SC PBE methods have underestimated the stability of 3D structures of Au_{12}^- and Au_8^+. SO TPSS and SO PBE methods may give the right 2D−3D transition point for the anionic and cationic gold clusters.

5. Conclusion

In the present work, we have systematically evaluated the performance of DFT functionals and the effect of SO coupling on the geometries and energetics of the Au_2, Au_3, Au_4, and Au_5 clusters. It was found that SO coupling has a significant effect on the cohesive energy and the relative stability of the isomers of gold clusters. Inclusion of SO coupling significantly increases the cohesive/atomization energy of the gold clusters. Except for a few functionals from the HCTH family, the SO correction to the atomization energy has a weak dependence on the choice of functionals. Interestingly, a good linear relationship (eq 6) between the SO correction to the atomization energy and the number of gold atoms and Au−Au bonds in the cluster has been found. The equation indicates that inclusion of SO coupling prefers the structure with more Au−Au bonds. It was also found that many functionals give the wrong stability order for the two isomers of Au_3, and the inclusion of SO coupling greatly remedies this. In the case of Au_4, the relative energies of the three isomers calculated by the SO DFT methods are closer to the values calculated by the SC CCSD(T) method.

The effect of the HF exchange in the DFT functionals has also been investigated. It was found that inclusion of HF exchange underestimates the cohesive energy of small gold clusters with or without SO coupling. A linear relationship is found between the cohesive energy of gold clusters and the proportion of the HF exchange included in the functionals.

The overall performance of different types of functionals has been evaluated. On average, GGA functionals are inferior to meta-GGA functionals in the calculations of cohesive energy and RE whether SO coupling is considered or not. Since inclusion of SO coupling overestimates the cohesive energy while inclusion of HF exchange underestimate the cohesive energy, this provides us a guideline to find a functional with good performance in the calculation of cohesive energies and relative energies of gold clusters, that is, a hybrid meta-GGA functional with SO coupling considered. In the present study, it was found that SO TPSSh has the best overall performance, while SC M06-L also performs reasonably well.

Acknowledgment. This work was supported by the National Science Foundations of China (20828003, 20973041) and the National Major Basic Research Program of China (2009CB623506, 2011CB808505).

Supporting Information Available: Atomization energy of Au_2, cohesive energy, and RE of Au_3 calculated by different DFT functionals not discussed in the text. Computational costs of the single-point calculations of the SO DFT methods for Au_2 and Au_3. The energy of tetrahedron Au_4 relative to that of rhombus Au_4 using different basis sets. This material is available free of charge via the Internet at http://pubs.acs.org.

References and Notes

(1) Pyykko, P. *Angew. Chem., Int. Ed.* **2004**, *43* (34), 4412–4456.
(2) Pyykko, P. *Inorg. Chim. Acta* **2005**, *358* (14), 4113–4130.
(3) Pyykko, P. *Chem. Soc. Rev.* **2008**, *37* (9), 1967–1997.
(4) Rousseau, R.; Dietrich, G.; Kruckeberg, S.; Lutzenkirchen, K.; Marx, D.; Schweikhard, L.; Walther, C. *Chem. Phys. Lett.* **1998**, *295* (1−2), 41–46.
(5) Mejias, J. A. *Phys. Rev. B* **1996**, *53* (15), 10281–10288.
(6) Sanchez, A.; Abbet, S.; Heiz, U.; Schneider, W. D.; Hakkinen, H.; Barnett, R. N.; Landman, U. *J. Phys. Chem. A* **1999**, *103* (48), 9573–9578.
(7) Hakkinen, H.; Abbet, W.; Sanchez, A.; Heiz, U.; Landman, U. *Angew. Chem., Int. Ed.* **2003**, *42* (11), 1297–1300.
(8) Perez-Jimenez, A. J.; Palacios, J. J.; Louis, E.; Sanfabian, E.; Verges, J. A. *ChemPhysChem* **2003**, *4* (4), 388–392.
(9) Han, Y. K. *J. Chem. Phys.* **2006**, *124* (2), 024316.
(10) Xiao, L.; Tollberg, B.; Hu, X. K.; Wang, L. C. *J. Chem. Phys.* **2006**, *124*, 114309.
(11) Xiao, L.; Wang, L. C. *Chem. Phys. Lett.* **2004**, *392* (4−6), 452–455.
(12) Bravo-Perez, G.; Garzon, I. L.; Novaro, O. *J. Mol. Struct.* **1999**, *493*, 225–231.
(13) Bravo-Perez, G.; Garzon, I. L.; Novaro, O. *Chem. Phys. Lett.* **1999**, *313* (3−4), 655–664.
(14) Olson, R. M.; Varganov, S.; Gordon, M. S.; Metiu, H.; Chretien, S.; Piecuch, P.; Kowalski, K.; Kucharski, S. A.; Musial, M. *J. Am. Chem. Soc.* **2005**, *127* (3), 1049–1052.
(15) Wilson, N. T.; Johnston, R. L. *Eur. Phys. J. D* **2000**, *12* (1), 161–169.
(16) Michaelian, K.; Rendon, N.; Garzon, I. L. *Phys. Rev. B* **1999**, *60* (3), 2000–2010.
(17) Balasubramanian, K.; Liao, D. W. *J. Chem. Phys.* **1991**, *94* (7), 5233–5236.
(18) Wang, J. L.; Wang, G. H.; Zhao, J. J. *Phys. Rev. B* **2002**, *66* (3), 035418.
(19) Hakkinen, H.; Landman, U. *Phys. Rev. B* **2000**, *62* (4), R2287–R2290.
(20) Remacle, F.; Kryachko, E. S. *Adv. Quantum Chem.* **2004**, *47*, 423–464.
(21) Remacle, F.; Kryachko, E. S. *J. Chem. Phys.* **2005**, *122* (4), 044304.
(22) Walker, A. V. *J. Chem. Phys.* **2005**, *122* (9), 094310.
(23) Fernandez, E. M.; Soler, J. M.; Balbas, L. C. *Phys. Rev. B* **2006**, *73* (23), 235433.
(24) Fernandez, E. M.; Soler, J. M.; Garzon, I. L.; Balbas, L. C. *Phys. Rev. B* **2004**, *70* (16), 165403.
(25) Bonacic-Koutecky, V.; Burda, J.; Mitric, R.; Ge, M. F.; Zampella, G.; Fantucci, P. *J. Chem. Phys.* **2002**, *117* (7), 3120–3131.
(26) Gronbeck, H.; Broqvist, P. *Phys. Rev. B* **2005**, *71* (7), 073408.
(27) Gronbeck, H.; Andreoni, W. *Chem. Phys.* **2000**, *262* (1), 1–14.
(28) Gilb, S.; Weis, P.; Furche, F.; Ahlrichs, R.; Kappes, M. M. *J. Chem. Phys.* **2002**, *116* (10), 4094–4101.
(29) Furche, F.; Ahlrichs, R.; Weis, P.; Jacob, C.; Gilb, S.; Bierweiler, T.; Kappes, M. M. *J. Chem. Phys.* **2002**, *117* (15), 6982–6990.
(30) Hakkinen, H.; Yoon, B.; Landman, U.; Li, X.; Zhai, H. J.; Wang, L. S. *J. Phys. Chem. A* **2003**, *107* (32), 6168–6175.
(31) Lee, H. M.; Ge, M. F.; Sahu, B. R.; Tarakeshwar, P.; Kim, K. S. *J. Phys. Chem. B* **2003**, *107* (37), 9994–10005.
(32) Gronbeck, H.; Broqvist, P. *Phys. Rev. B* **2005**, *71* (7), 205428.
(33) Fa, W.; Luo, C. F.; Dong, J. M. *Phys. Rev. B* **2005**, *72* (20), 205428.
(34) Fa, W.; Dong, J. M. *J. Chem. Phys.* **2006**, *124* (11), 114310.
(35) Diefenbach, M.; Kim, K. S. *J. Phys. Chem. B* **2006**, *110*, 21639–21642.
(36) Yoon, B.; Koskinen, P.; Huber, B.; Kostko, O.; von Issendorff, B.; Hakkinen, H.; Moseler, M.; Landman, U. *ChemPhysChem* **2007**, *8*, 157–161.
(37) Bulusu, S.; Li, X.; Wang, L. S.; Zeng, X. C. *J. Phys. Chem. C* **2007**, *111* (11), 4190–4198.
(38) Gu, X.; Bulusu, S.; Li, X.; Zeng, X. C.; Li, J.; Gong, X. G.; Wang, L. S. *J. Phys. Chem. C* **2007**, *111* (23), 8228–8232.

(39) Kryachko, E. S.; Remacle, F. *Int. J. Quantum Chem.* **2007**, *107* (14), 2922–2934.
(40) Lechtken, A.; Schooss, D.; Stairs, J. R.; Blom, M. N.; Furche, F.; Morgner, N.; Kostko, O.; von Issendorff, B.; Kappes, M. M. *Angew. Chem., Int. Ed.* **2007**, *46* (16), 2944–2948.
(41) Crespo, O.; Laguna, A.; Fernandez, E. J.; Lopez-de-Luzuriaga, J. M.; Jones, P. G.; Teichert, M.; Monge, M.; Pyykko, P.; Runeberg, N.; Schutz, M.; Werner, H. J. *Inorg. Chem.* **2000**, *39* (21), 4786–4792.
(42) Schwerdtfeger, P.; Hermann, H. L.; Schmidbaur, H. *Inorg. Chem.* **2003**, *42* (4), 1334–1342.
(43) Schwerdtfeger, P.; Boyd, P. D. W.; Burrell, A. K.; Robinson, W. T.; Taylor, M. J. *Inorg. Chem.* **1990**, *29* (18), 3593–3607.
(44) Quinn, B. M.; Liljeroth, P.; Ruiz, V.; Laaksonen, T.; Kontturi, K. *J. Am. Chem. Soc.* **2003**, *125* (22), 6644–6645.
(45) Hakkinen, H.; Barnett, R. N.; Landman, U. *J. Phys. Chem. B* **1999**, *103* (42), 8814–8816.
(46) Kruger, D.; Rousseau, R.; Fuchs, H.; Marx, D. *Angew. Chem., Int. Ed.* **2003**, *42* (20), 2251–2253.
(47) Tachibana, M.; Yoshizawa, K.; Ogawa, A.; Fujimoto, H.; Hoffmann, R. *J. Phys. Chem. B* **2002**, *106* (49), 12727–12736.
(48) Yourdshahyan, Y.; Rappe, A. M. *J. Chem. Phys.* **2002**, *117* (2), 825–833.
(49) Gao, Y.; Shao, N.; Zeng, X. C. *ACS Nano* **2008**, *2* (7), 1497–1503.
(50) Li, Y.; Galli, G.; Gygi, F. *ACS Nano* **2008**, *2* (9), 1896–1902.
(51) Schroder, D.; Schwarz, H.; Hrusak, J.; Pyykko, P. *Inorg. Chem.* **1998**, *37* (4), 624–632.
(52) Schwerdtfeger, P.; McFeaters, J. S.; Liddell, M. J.; Hrusak, J.; Schwarz, H. *J. Chem. Phys.* **1995**, *103* (1), 245–252.
(53) Hrusak, J.; Hertwig, R. H.; Schroder, D.; Schwerdtfeger, P.; Koch, W.; Schwarz, H. *Organometallics* **1995**, *14* (3), 1284–1291.
(54) Schroder, D.; Hrusak, J.; Hertwig, R. H.; Koch, W.; Schwerdtfeger, P.; Schwarz, H. *Organometallics* **1995**, *14* (1), 312–316.
(55) Komarov, P. V.; Zherenkova, L. V.; Khalatur, P. G. *J. Chem. Phys.* **2008**, *128* (12), 124909.
(56) Ren, S. W. *Int. J. Mod. Phys. C* **2009**, *20* (5), 667–675.
(57) Verma, V.; Dharamvir, K. *J. Nano Res.* **2008**, *4*, 65–77.
(58) Rodrigues, D. D. C.; Nascimento, A. M.; Duarte, H. A.; Belchior, J. C. *Chem. Phys.* **2008**, *349* (1−3), 91–97.
(59) Foiles, S. M.; Baskes, M. I.; Daw, M. S. *Phys. Rev. B* **1986**, *33* (12), 7983–7991.
(60) Ercolessi, F.; Parrinello, M.; Tosatti, E. *Philos. Mag. A* **1988**, *58* (1), 213–226.
(61) Oh, D. J.; Johnson, R. A. *J. Mater. Res.* **1988**, *3* (3), 471–478.
(62) Ackland, G. J.; Vitek, V. *Phys. Rev. B* **1990**, *41* (15), 10324–10333.
(63) Cleri, F.; Rosato, V. *Phys. Rev. B* **1993**, *48* (1), 22–33.
(64) Kelchner, C. L.; Halstead, D. M.; Perkins, L. S.; Wallace, N. M.; Depristo, A. E. *Surf. Sci.* **1994**, *310* (1−3), 425–435.
(65) Cai, J.; Ye, Y. Y. *Phys. Rev. B* **1996**, *54* (12), 8398–8410.
(66) Kallinteris, G. C.; Papanicolaou, N. I.; Evangelakis, G. A.; Papaconstantopoulos, D. A. *Phys. Rev. B* **1997**, *55* (4), 2150–2156.
(67) Gupta, R. P. *Phys. Rev. B* **1981**, *23* (12), 6265–6270.
(68) Daw, M. S.; Baskes, M. I. *Phys. Rev. Lett.* **1983**, *50* (17), 1285–1288.
(69) Sutton, A. P.; Chen, J. *Philos. Mag. Lett.* **1990**, *61* (3), 139–146.
(70) Grochola, G.; Russo, S. P.; Snook, I. K. *J. Chem. Phys.* **2005**, *123* (20), 204719.
(71) Luo, S. N.; Ahrens, T. J.; Cagin, T.; Strachan, A.; Goddard, W. A.; Swift, D. C. *Phys. Rev. B* **2003**, *68* (13), 134206.
(72) Avinc, A.; Dimitrov, V. I. *Comput. Mater. Sci.* **1999**, *13* (4), 211–217.
(73) Bishea, G. A.; Morse, M. D. *J. Chem. Phys.* **1991**, *95* (8), 5646–5659.
(74) James, A. M.; Kowalczyk, P.; Simard, B.; Pinegar, J. C.; Morse, M. D. *J. Mol. Spectrosc.* **1994**, *168* (2), 248–257.
(75) Hilpert, K.; Gingerich, K. A. *Ber. Bunsen-Ges. Phys. Chem* **1980**, *84* (8), 739–745.
(76) Pyykko, P. *Angew. Chem., Int. Ed.* **2002**, *41* (19), 3573–3578.
(77) Desclaux, J. P.; Pyykko, P. *Chem. Phys. Lett.* **1976**, *39* (2), 300–303.
(78) Pyykko, P.; Desclaux, J. P. *Acc. Chem. Res.* **1979**, *12* (8), 276–281.
(79) Pyykko, P. *Chem. Rev.* **1988**, *88* (3), 563–594.
(80) Christensen, N. E.; Seraphin, B. O. *Phys. Rev. B* **1971**, *4* (10), 3321–3344.
(81) Engel, E.; Dreizler, R. Relativistic Density Functional Theory. In *Density Functional Theory II*; Springer: Berlin, Germany, 1996; Vol. 181, pp 1−80.
(82) Kullie, O.; Zhang, H.; Kolb, D. *Chem. Phys.* **2008**, *351* (1−3), 106–110.
(83) Bylaska, E. J.; Govind, W. A. d. J. N.; Kowalski, K.; Straatsma, T. P.; Valiev, M.; Wang, D.; Apra, E.; Windus, T. L.; Hammond, J.; Nichols, P.; Hirata, S.; Hackler, M. T.; Zhao, Y.; Fan, P. D.; Harrison, R. J.; Dupuis, M.; Smith, D. M. A.; Nieplocha, M.; Tipparaju, V.; Krishnan, M.; Wu, Q.; Van Voorhis, T.; Auer, A. A.; Nooijen, M.; Brown, E.; Cisneros, G.; Fann, G. I.; Fruchtl, H.; Garza, J.; Hirao, K.; Kendall, R.; Nichols, J. A.; Tsemekhman, K.; Wolinski, K.; Anchell, J.; Bernholdt, D.; Borowski, P.; Clark, T.; Clerc, D.; Dachsel, H.; Deegan, M.; Dyall, K.; Elwood, D.; Glendening, E.; Gutowski, M.; Hess, A.; Jaffe, J.; Johnson, B.; Ju, J.; Kobayashi, R.; Kutteh, R.; Lin, Z.; Littlefield, R.; Long, X.; Meng, B.; Nakajima, T.; Niu, S.; Pollack, L.; Rosing, M.; Sandrone, G.; Stave, M.; Taylor, H.; Thomas, G.; van Lenthe, J.; Wong, A.; Zhang, Z. *NWChem, A Computational Chemistry Package for Parallel Computers*, Version 5.1; Pacific Northwest National Laboratory: Richland, WA, 2007.
(84) Kendall, R. A.; Apra, E.; Bernholdt, D. E.; Bylaska, E. J.; Dupuis, M.; Fann, G. I.; Harrison, R. J.; Ju, J. L.; Nichols, J. A.; Nieplocha, J.; Straatsma, T. P.; Windus, T. L.; Wong, A. T. *Comput. Phys. Commun.* **2000**, *128* (1−2), 260–283.
(85) Ross, R. B.; Powers, J. M.; Atashroo, T.; Ermler, W. C.; Lajohn, L. A.; Christiansen, P. A. *J. Chem. Phys.* **1994**, *101* (11), 10198–10199.
(86) Rusakov, A. A.; Rykova, E.; Scuseria, G. E.; Zaitsevskii, A. *J. Chem. Phys.* **2007**, *127* (16), 164322.
(87) Fuentealba, P.; Simon-Manso, Y. *Chem. Phys. Lett.* **1999**, *314* (1−2), 108–113.
(88) Gruene, P.; Rayner, D. M.; Redlich, B.; van der Meer, A. F. G.; Lyon, J. T.; Meijer, G.; Fielicke, A. *Science* **2008**, *321* (5889), 674–676.
(89) Assadollahzadeh, B.; Schwerdtfeger, P. *J. Chem. Phys.* **2009**, *131* (6), 064306.
(90) Bulusu, S.; Zeng, X. C. *J. Chem. Phys.* **2006**, *125* (15), 154303.
(91) Li, X. B.; Wang, H. Y.; Yang, X. D.; Zhu, Z. H.; Tang, Y. J. *J. Chem. Phys.* **2007**, *126* (8), 084505.
(92) Olson, R. M.; Gordon, M. S. *J. Chem. Phys.* **2007**, *126* (21), 214310.
(93) Gruber, M.; Heimel, G.; Romaner, L.; Bredas, J. L.; Zojer, E. *Phys. Rev. B* **2008**, *77* (16), 165411.
(94) Peterson, K. A.; Puzzarini, C. *Theor. Chem. Acc.* **2005**, *114* (4−5), 283–296.
(95) Wesendrup, R.; Hunt, T.; Schwerdtfeger, P. *J. Chem. Phys.* **2000**, *112* (21), 9356–9362.
(96) Becke, A. D. *Phys. Rev. A* **1988**, *38* (6), 3098–3100.
(97) Lee, C. T.; Yang, W. T.; Parr, R. G. *Phys. Rev. B* **1988**, *37* (2), 785–789.
(98) Perdew, J. P. *Phys. Rev. B* **1986**, *33* (12), 8822–8824.
(99) Perdew, J. P.; Burke, K.; Ernzerhof, M. *Phys. Rev. Lett.* **1996**, *77* (18), 3865–3868.
(100) Perdew, J. P.; Burke, K.; Ernzerhof, M. *Phys. Rev. Lett.* **1997**, *78* (7), 1396–1396.
(101) Perdew, J. P.; Wang, Y. *Phys. Rev. B* **1992**, *45* (23), 13244–13249.
(102) Filatov, M.; Thiel, W. *Mol. Phys.* **1997**, *91* (5), 847–859.
(103) Filatov, M.; Thiel, W. *Int. J. Quantum Chem.* **1997**, *62* (6), 603–616.
(104) Hamprecht, F. A.; Cohen, A. J.; Tozer, D. J.; Handy, N. C. *J. Chem. Phys.* **1998**, *109* (15), 6264–6271.
(105) Boese, A. D.; Doltsinis, N. L.; Handy, N. C.; Sprik, M. *J. Chem. Phys.* **2000**, *112* (4), 1670–1678.
(106) Boese, A. D.; Handy, N. C. *J. Chem. Phys.* **2001**, *114* (13), 5497–5503.
(107) Menconi, G.; Wilson, P. J.; Tozer, D. J. *J. Chem. Phys.* **2001**, *114* (9), 3958–3967.
(108) Boese, A. D.; Chandra, A.; Martin, J. M. L.; Marx, D. *J. Chem. Phys.* **2003**, *119* (12), 5965–5980.
(109) Tsuneda, T.; Suzumura, T.; Hirao, K. *J. Chem. Phys.* **1999**, *110* (22), 10664–10678.
(110) Tsuneda, T.; Suzumura, T.; Hirao, K. *J. Chem. Phys.* **1999**, *111* (13), 5656–5667.
(111) Cohen, A. J.; Handy, N. C. *Chem. Phys. Lett.* **2000**, *316* (1−2), 160–166.
(112) Stephens, P. J.; Devlin, F. J.; Chabalowski, C. F.; Frisch, M. J. *J. Phys. Chem.* **1994**, *98* (45), 11623–11627.
(113) Becke, A. D. *J. Chem. Phys.* **1993**, *98* (7), 5648–5652.
(114) Becke, A. D. *J. Chem. Phys.* **1993**, *98* (2), 1372–1377.
(115) Becke, A. D. *J. Chem. Phys.* **1997**, *107* (20), 8554–8560.
(116) Wilson, P. J.; Bradley, T. J.; Tozer, D. J. *J. Chem. Phys.* **2001**, *115* (20), 9233–9242.
(117) Keal, T. W.; Tozer, D. J. *J. Chem. Phys.* **2005**, *123* (12), 121103.
(118) Schmider, H. L.; Becke, A. D. *J. Chem. Phys.* **1998**, *108* (23), 9624–9631.
(119) Adamo, C.; Barone, V. *J. Chem. Phys.* **1999**, *110* (13), 6158–6170.
(120) Lynch, B. J.; Fast, P. L.; Harris, M.; Truhlar, D. G. *J. Phys. Chem. A* **2000**, *104* (21), 4811–4815.
(121) Zhao, Y.; Truhlar, D. G. *J. Chem. Phys.* **2006**, *125* (19), 194101.
(122) Tao, J. M.; Perdew, J. P.; Staroverov, V. N.; Scuseria, G. E. *Phys. Rev. Lett.* **2003**, *91* (14), 146301.

(123) Perdew, J. P.; Kurth, S.; Zupan, A.; Blaha, P. *Phys. Rev. Lett.* **1999**, *82* (12), 2544–2547.
(124) Zhao, Y.; Schultz, N. E.; Truhlar, D. G. *J. Chem. Phys.* **2005**, *123* (16), 161103.
(125) Zhao, Y.; Schultz, N. E.; Truhlar, D. G. *J. Chem. Theory Comput.* **2006**, *2* (2), 364–382.
(126) Zhao, Y.; Truhlar, D. G. *J. Phys. Chem. A* **2006**, *110* (49), 13126–13130.
(127) Van Voorhis, T.; Scuseria, G. E. *J. Chem. Phys.* **1998**, *109* (2), 400–410.
(128) Zhao, Y.; Truhlar, D. G. *J. Phys. Chem. A* **2004**, *108* (33), 6908–6918.
(129) Zhao, Y.; Truhlar, D. G. *J. Phys. Chem. A* **2005**, *109* (25), 5656–5667.
(130) Zhao, Y.; Lynch, B. J.; Truhlar, D. G. *J. Phys. Chem. A* **2004**, *108* (14), 2715–2719.
(131) Staroverov, V. N.; Scuseria, G. E.; Tao, J. M.; Perdew, J. P. *J. Chem. Phys.* **2003**, *119* (23), 12129–12137.
(132) Christiansen, P. A.; Lee, Y. S.; Pitzer, K. S. *J. Chem. Phys.* **1979**, *71* (11), 4445–4450.
(133) Lee, Y. S.; Ermler, W. C.; Pitzer, K. S. *J. Chem. Phys.* **1977**, *67* (12), 5861–5876.
(134) Kahn, L. R.; Baybutt, P.; Truhlar, D. G. *J. Chem. Phys.* **1976**, *65* (10), 3826–3853.
(135) Chang, A. H. H.; Pitzer, R. M. *J. Am. Chem. Soc.* **1989**, *111* (7), 2500–2507.
(136) Wang, F.; Liu, W. J. *Chem. Phys.* **2005**, *311* (1−2), 63–69.
(137) Lee, Y. S.; Ermler, W. C.; Pitzer, K. S.; McLean, A. D. *J. Chem. Phys.* **1979**, *70* (1), 288–292.
(138) Fabiano, E.; Piacenza, M.; Della Sala, F. *Phys. Chem. Chem. Phys.* **2009**, *11* (40), 9160–9169.
(139) Balasubramanian, K.; Liao, M. Z. *J. Chem. Phys.* **1987**, *86* (10), 5587–5590.
(140) Feller, D. *J. Chem. Phys.* **1992**, *96* (8), 6104–6114.
(141) Feller, D. *J. Chem. Phys.* **1993**, *98* (9), 7059–7071.
(142) Mantina, M.; Valero, R.; Truhlar, D. G. *J. Chem. Phys.* **2009**, *131* (6), 064706.
(143) Ferrighi, L.; Hammer, B.; Madsen, G. K. H. *J. Am. Chem. Soc.* **2009**, *131* (30), 10605–10609.
(144) Schaftenaar, G.; Noordik, J. H. *J. Comput. Aided Mol. Des.* **2000**, *14* (2), 123–134.
(145) Huber, K. P.; Herzberg, G. *Constants of Diatomic Molecules*; Van Nostrand-Reinhold: New York, 1979.

JP105428B